

Supplementary Information for

Engineering a potent receptor superagonist or antagonist from a novel IL-6 family cytokine ligand

Jun W. Kim, Cesar P. Marquez, R. Andres Parra Sperberg, Jiaxiang Wu, Won G. Bae, Po-Ssu Huang, E. Alejandro Sweet-Cordero and Jennifer R. Cochran

* E. Alejandro Sweet-Cordero, Jennifer R. Cochran

Email: alejandro.sweet-cordero@ucsf.edu or jennifer.cochran@stanford.edu

This PDF file includes:

Figures S1 to S6

Tables S1 to S2

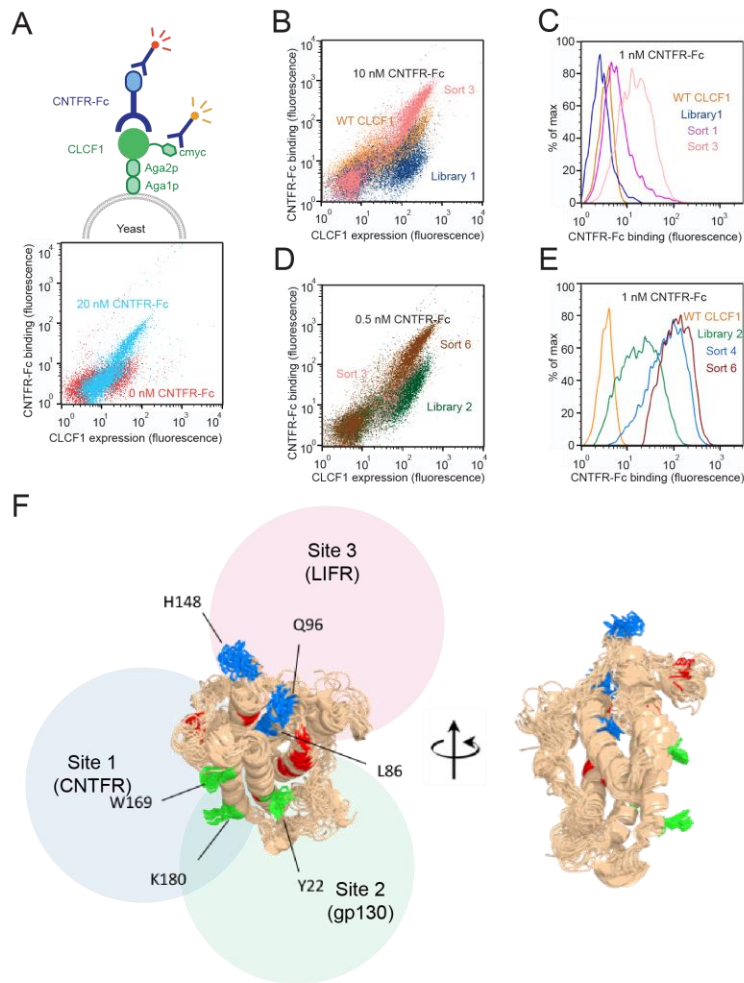


Fig. S1. CLCF1 engineering strategy. (A) Wild-type CLCF1 (WT CLCF1) was expressed on the yeast cell surface as a fusion to the agglutinin mating protein Aga2p and was shown to bind to soluble CNTFR (CNTFR-Fc). The overlaid flow cytometry dot plot represents CLCF1 expression levels on the yeast cell surface (x-axis), and binding with (cyan) and without (red) 20 nM CNTFR-Fc (y-axis). (B) CLCF1 library created by error-prone PCR was sorted three times with FACS using 20 nM, 2 nM, and 0.5 nM CNTFR-Fc, each time isolating yeast displaying CLCF1 variants with increased binding affinity. (C) The overlaid flow cytometry dot plot represents binding of yeast-displayed wild-type CLCF1 (orange) and unsorted library 1 (blue) to 10 nM CNTFR-Fc. (D) Second-generation CLCF1 library created by DNA shuffling (StEP) was sorted with FACS once using 0.5 nM CNTFR-Fc (sort 4) and twice using a kinetic off-rate method where CNTFR-Fc (2 nM) bound yeast were washed to remove unbound CNTFR-Fc, and incubated for 10 h (sort 5) and 24 h (sort 6) before FACS sorting. The overlaid flow cytometry dot plot represents binding of yeast-displayed sort 3 products from library 1 (pink) and unsorted library 2 (green) to 0.5 nM CNTFR-Fc. (E) Flow cytometry histograms depicting binding of the starting library, wild-type CLCF1, and the intermediate sort products to 1 nM CNTFR-Fc. (F) Using a deep learning based prediction a total of 5000 modeled CLCF1 structures were generated, from which the 500 lowest energy

structures were selected by total Rosetta energy. Structures were further selected by disulfide energy (dsf_fal13), resulting in an ensemble of 20 lowest disulfide energy structures as shown.

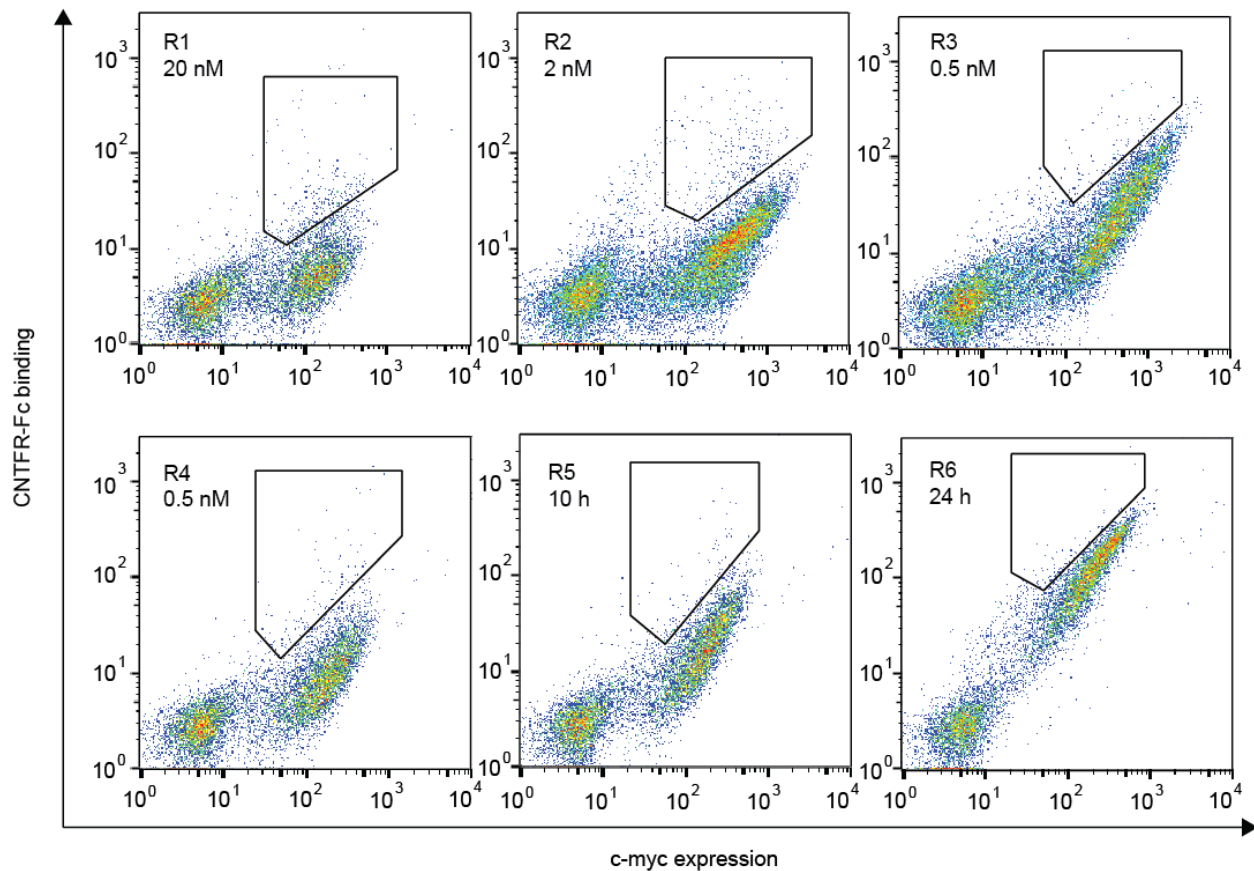
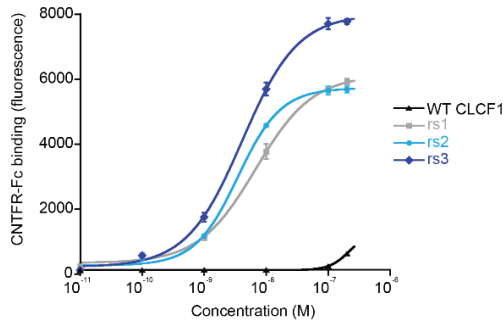


Fig. S2. Library sort progressions. Flow cytometry dot plots indicating Alexa-488 for CNTFR-Fc binding (y-axis) and PE fluorescence for anti-cmyc expression (x-axis) on a single-cell level. Yeast-displayed CLCF1 libraries were screened by multi-color FACS for mutants that bound the most CNTFR-Fc for a given amount of expression. The initial library (library 1) was created using random mutagenesis achieved via error-prone PCR and sorted using equilibrium binding conditions. CNTFR-Fc concentrations were reduced in successive rounds of sorting from 20 nM (R1), to 2 nM (R2), and 0.5 nM (R3). The second library (library 2) was created using staggered extension process (StEP) and sorted following equilibrium binding of 0.5 nM CNTFR-Fc (R4), or using a kinetic off-rate method where CNTFR-Fc (2 nM) bound yeast were washed to remove unbound CNTFR-Fc, and incubated for 10 h (R5) and 24 h (R6) before FACS sorting

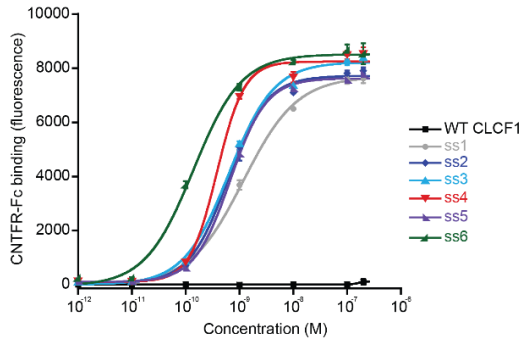
A



B

	Residue no.			CNTFR
	86	96	148	Affinity
WT	L	Q	H	K_d (nM)
rs1		R		8 ± 2
rs2	F	R		3.1 ± 0.1
rs3		R	R	4.2 ± 0.3

C



D

	Residue no.						CNTFR
	22	86	96	148	169	180	Affinity
WT	Y	L	Q	H	W	K	K_d (pM)
ss1		F	R	R			830 ± 30
ss2		F	R	R	L		220 ± 20
ss3		F	R	R		R	280 ± 30
ss4		F	R	R	L	R	80 ± 20
ss5	C	F	R	R			180 ± 70
ss6	C	F	R	R	L	R	60 ± 10

Fig. S3. Binding characterization of yeast-displayed CLCF1 variants from affinity maturation. (A) Yeast displaying CLCF1 variants isolated from library 1 screening were incubated with varying concentrations of CNTFR-Fc. (B) Equilibrium binding (K_d) values of yeast displaying CLCF1 variants from library 1 for CNTFR-Fc. The K_d value of WT CLCF1 could not be quantified due to low binding affinity. (C) Yeast displaying CLCF1 variants isolated from library 2 screening were incubated with varying concentrations of CNTFR-Fc. (D) Equilibrium binding (K_d) values of yeast displaying CLCF1 variants from library 2 for CNTFR-Fc. Secondary labeling was performed using anti-mouse Fc antibody and anti-cmyc antibody to detect CNTFR-Fc binding and cell surface expression, respectively. CNTFR-Fc binding was quantified only in the gated population of yeast expressing CLCF1 variants. Error bars represent \pm standard deviation of three measurements.

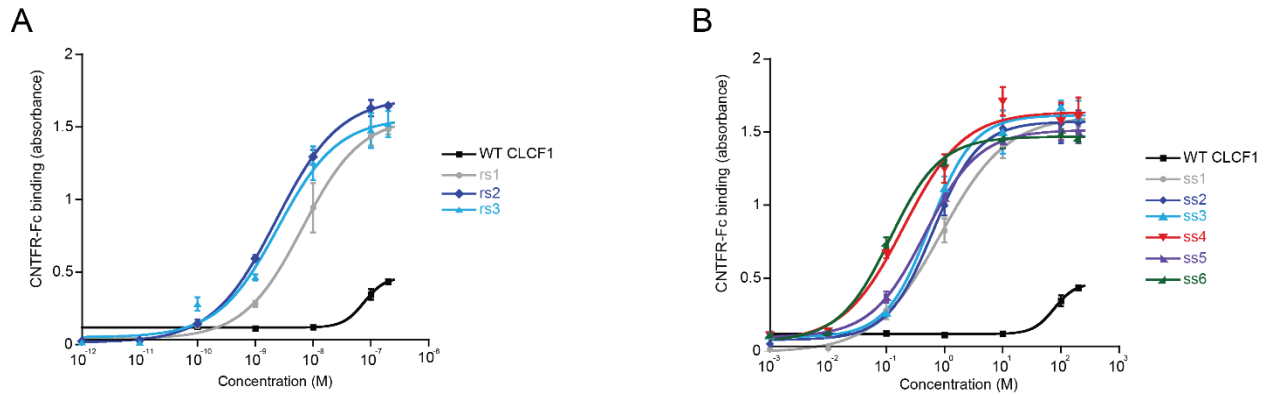


Fig. S4. Binding characterization of CLCF1 variants produced as soluble proteins. (A) Binding of CLCF1 variants from library 1 with CNTFR-Fc. (B) Binding of CLCF1 variants from library 2 with CNTFR-Fc. Values were measured with an ELISA-based assay, where an anti-Fc antibody was used to capture the CLCF1/CNTFR-Fc complex, and an anti-CLCF1 antibody was used as a detection agent. Apparent K_d values are shown in Fig. 1C. Consistent with the results from yeast cell surface binding assay, the affinity of WT CLCF1 was too weak to allow quantification of a K_d value. Error bars represent \pm standard deviation of three measurements.

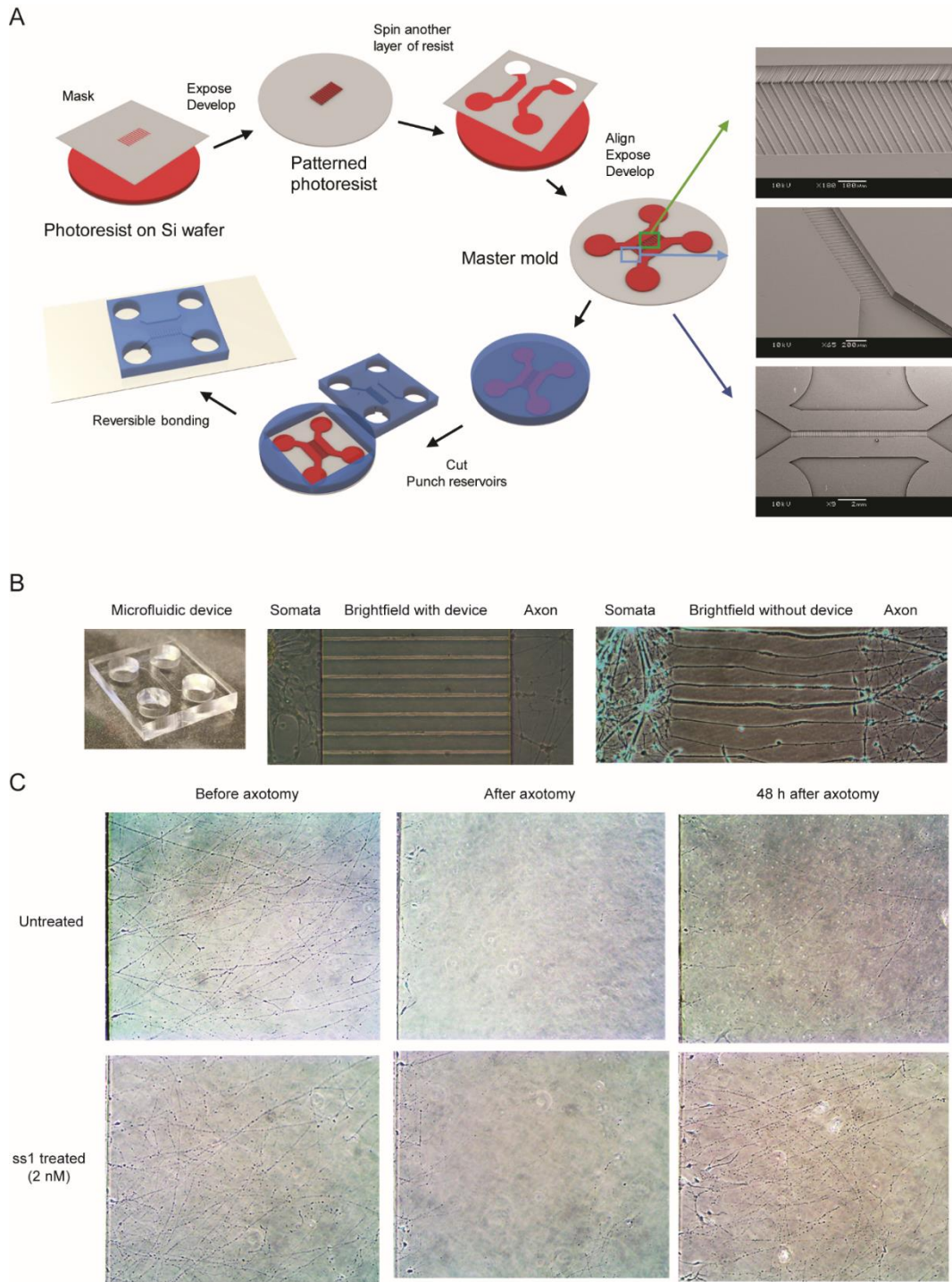


Fig. S5. Microfluidic device for axonal injury model. (A) Schematic showing fabrication process of a microfluidic device that enables directional axonal growth. (B) Rat embryonic neurons (E18) were cultured in the somata chamber allowing isolation of axons through the microgrooves. The device was removed without major alteration of the cell arrangement. (C) Axotomy was performed after allowing cells to grow for 4 days. Injured cells treated with ss1 showed substantially higher regrowth of axons 48 hours after axotomy compared to untreated control.

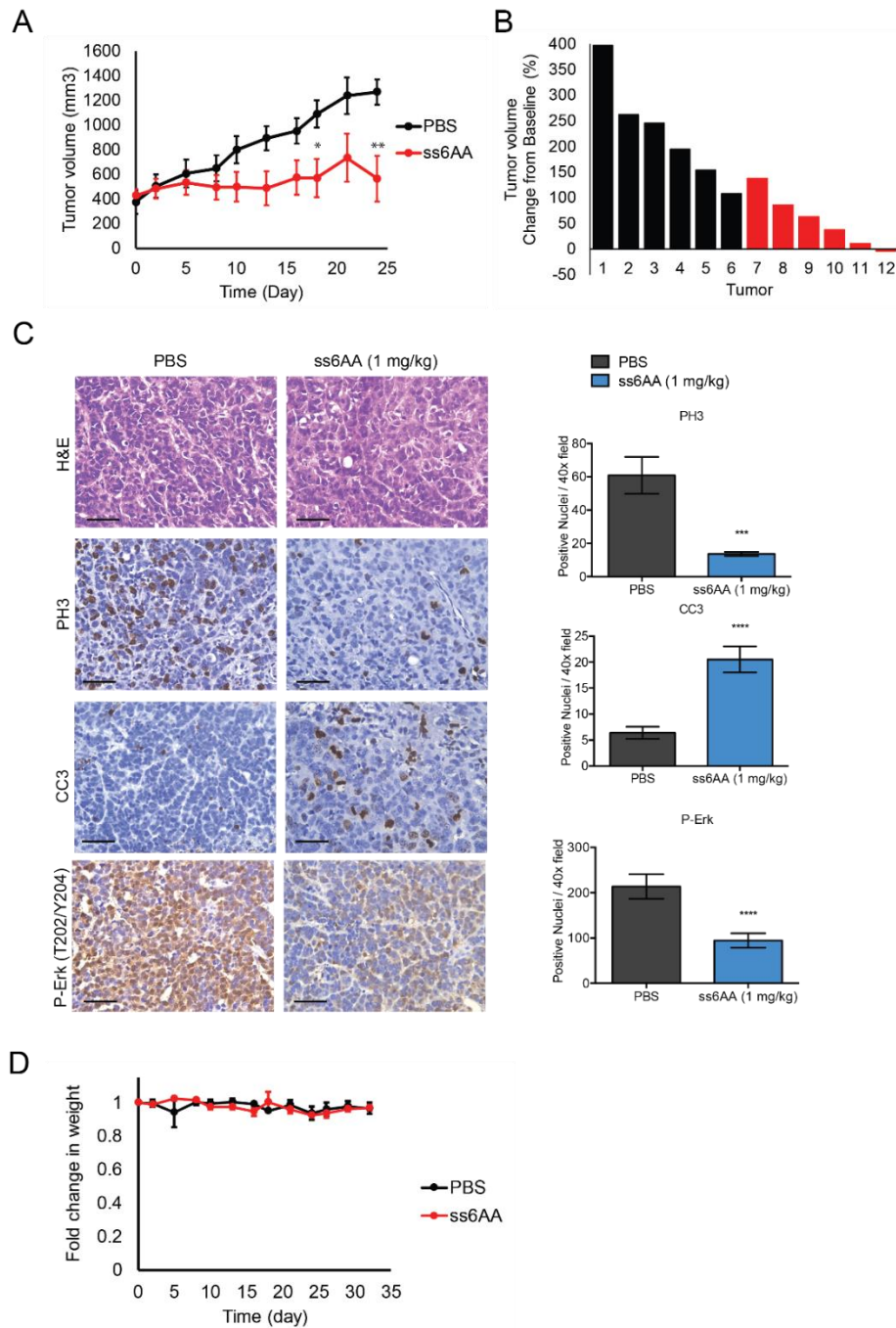


Fig. S6. ss6AA treatment inhibits H23 xenograft tumor growth *in vivo*. (A) Mice bearing H23 tumors in both flanks were treated with 1 mg kg⁻¹ body weight ss6AA or phosphate buffered saline three times per week for 3 weeks. Error bars represent \pm s.e., n = 6 per treatment; * P < 0.05, ** P < 0.01, *** P < 0.001. (B) Waterfall plot of individual tumors on day 24 post treatment. (C) Representative hematoxylin and eosin (H&E) staining and immunohistochemistry for phospho-histone H3 (PH3), cleaved caspase (CC3), and phospho-Erk (P-Erk) from H23 xenografts. Scale bars, 50 μ m. Quantified values were compared using one-way ANOVA. Error bars represent \pm s.e. (D) Fold change in body weight of mice (n = 3) treated with ss6AA or saline.

Table S1. Sequences of CLCF1 clones randomly selected following sort 3 of library 1. DNA from twenty yeast colonies were sequenced at random from the pool of CLCF1 variants recovered from sort 3 of library 1. Amino acid mutations and the relative wild-type residues are indicated. Q96R was the most highly observed mutation throughout the sequenced clones. L86F and H148R, although not as frequent as Q96R, also increased CNTFR affinity as shown in Fig.1. and Fig. S3.

Residue no.	8	25	32	55	62	69	71	74	86	88	96	99	107	108	112	119	133	142	148	156	158	162	166	169	173	179	180	183	184	189	
WT	P	H	G	E	V	S	S	L	L	C	Q	T	A	H	S	S	Q	W	H	D	F	K	T	W	K	K	K	Q	P	V	
Clone 1											R																				
Clone 2								Q											R					L							
Clone 3							S				R									E											
Clone 4											R																				
Clone 5		Y									R				G																
Clone 6											R											S									
Clone 7											R																				
Clone 8	T					G			F		R			R		N															
Clone 9											R									R											
Clone 10											R																				
Clone 11										W	R									R											
Clone 12										R	R																			S	
Clone 13			R								R																R				
Clone 14		R							F		R																			L	
Clone 15				G							R																			R	
Clone 16											R																				
Clone 17											R																				
Clone 18											R																				
Clone 19									F		R																				
Clone 20											R																				

Table S2. Sequences of CLCF1 clones randomly selected following sort 3 of library 2. DNA from twenty-two yeast colonies were sequenced at random from the pool of CLCF1 variants recovered from sort 3 of library 2. Amino acid mutations and the relative wild-type residues are indicated. In addition to Q96R, L86F and H148R, two additional mutations (W169L and K180R) were found to be enriched following screening. Although not observed as frequently, Y22C also slightly increased CNTFR affinity and decreased gp130 binding as shown in Fig. 1 and Fig. S3.

Residue no.	7	22	25	32	62	71	74	86	88	96	111	112	133	139	142	148	151	152	156	158	162	169	180	183	
WT	P	Y	H	H	V	N	L	L	C	Q	T	S	Q	E	W	H	F	S	D	F	K	W	K	Q	
Clone 1					I					R			R			R							L		
Clone 2		C					Q									R							L	R	
Clone 3										R		G			S		S						L	R	
Clone 4										R		R									R				
Clone 5						S				R						R							L	R	
Clone 6			Y					F		R		G			S					Y				R	
Clone 7						S				R														R	
Clone 8			R	R				F		R	A					R							L		
Clone 9					I				R	R					S								L	R	
Clone 10		C						F		R			G											R	
Clone 11					I		Q			R											R			R	
Clone 12						S		F		R														R	L
Clone 13					I					R													L		
Clone 14					R			F		R								G					L		
Clone 15						I				R						R							L		
Clone 16					R			F		R											R			R	
Clone 18							Q									R							L	R	R
Clone 19								F		R						R							L		L
Clone 20									R	R		G							E				L		
Clone 21	T					S		F		R						R							L		
Clone 22			R					F		R												R			L

Dataset S1. Ensemble of 20 lowest energy CLCF1 models.

Dataset S2. CNTFR, LIFR, and gp130 in complex with 3 lowest energy CLCF1 models.